Available online at www.sciencedirect.com

ScienceDirect

ELSEVIER

Nuclear and Particle Physics Proceedings 273–275 (2016) 2542–2544

www.elsevier.com/locate/nppp

Muon momentum scale and resolution in pp collisions at $\sqrt{s} = 8$ TeV in ATLAS

G. Artoni[a], on behalf of the ATLAS Collaboration

[a] *Brandeis University, 415 South Street, Waltham, MA 02453*

Abstract

This work shows the performance in the muon momentum scale and resolution achieved by ATLAS during the 2012 run at $\sqrt{s} = 8$. The momentum scale is known with an uncertainty ranging from 0.05% (in the central rapidity region) to 0.2% (at large rapidities). The muon momentum resolution is measured to be 1.7% for central muons with low momentum ($p_T \simeq 10$ GeV) and reaches 4% for high-p_T muons in the forward regions of the ATLAS detector.

1. Introduction

Muons are used in a very wide range of measurements by the ATLAS experiment [1] and hence the knowledge of their momenta is a fundamental ingredient to physics analyses. In particular, the muon momentum scale and resolution are crucial for the measurement of the Higgs boson mass [2]. A detailed overview of the performance of the ATLAS muon reconstruction for 2011 and 2012 collision data can be found in Ref.[3].

The ATLAS experiment uses mainly information from two sub-detectors, the Inner Detector (ID) and the Muon Spectrometer (MS), to efficiently reconstruct muons. The Inner Detector reconstructs the tracks associated to charged particles by combining high-resolution detectors at inner radii with continuous tracking at outer radii. It is contained in a solenoidal magnetic field of 2 T and its acceptance is $|\eta| < 2.5$. The Muon Spectrometer is designed for muon detection within $|\eta| < 2.7$. Three large air core toroidal magnets with a mean magnetic field of 0.5 T allow for a precise measurement of muon momenta up to the TeV range. According to the available information from the various sub-detectors, muons are reconstructed following specific criteria which lead to different muon classes. The muon types used in this article are:

- Stand-Alone muons: the muon track has been reconstructed only using the MS and its parameters are estimated by extrapolating it to the primary interaction vertex. They are used when the muon falls outside the coverage of the ID ($2.5 < |\eta| < 2.7$).
- Combined muons: the main type of muons is obtained by combining the tracks coming from the ID and MS, which are reconstructed separately.
- Segment-tagged muons: an ID track is considered to be a muon if it matches local track segments in the MS. This type is especially useful to recover acceptance for muons which fall in MS regions with smaller acceptance or that traverse less chambers due to their low momentum.

2. Corrections to the simulated muon momentum

The ATLAS simulation includes the best knowledge of the detector geometry, material budget and modelling of muon interactions available at the time of its production and needs additional corrections in order to reproduce the muon momentum scale and resolution observed in data. We correct separately the ID and MS tracks of a single muon using this equation:

$$(p_{\mathrm{T}}^{\mathrm{det}})' = \frac{p_{\mathrm{T}}^{\mathrm{det}} + \sum_{n=0}^{1} s_n^{\mathrm{det}}(\eta,\phi)\cdot(p_{\mathrm{T}}^{\mathrm{det}})^n}{1 + \sum_{m=0}^{2} g_m \Delta r_m^{\mathrm{det}}(\eta,\phi)\cdot(p_{\mathrm{T}}^{det})^{m-1}} \quad (1)$$

where $p_{\mathrm{T}}^{\mathrm{det}}$ represents either the p_{T} measured in the ID or the p_{T} measured with the MS and g_m are random

http://dx.doi.org/10.1016/j.nuclphysbps.2015.09.453

variables following a standard normal distribution. The scale and smearing parameters (s_n and Δr_m, respectively) have to be determined from data.

2.1. Scale and smearing parameters

The meaning of the different parameters appearing in the empirical parametrisation of Eq.1 is the following:

- s_0 - This parameter accounts for energy loss in the calorimeter and in other materials. $s_0^{ID}=0$ since the energy loss between the interaction vertex and the ID is negligible.
- s_1 - Radial distortion of the detector and limited knowledge of the magnetic field integral are responsible for this correction which is proportional to the transverse momentum of the muon.
- Δr_0 - Fluctuations of the energy loss in the material can give rise to this term, inversely proportional to the transverse momentum. $\Delta r_0^{ID}=0$ since the material between the interaction vertex and the Inner Detector does not give rise to sizeable effects.
- Δr_1 - This correction term represents multiple scattering, local inhomogeneities of the magnetic field as well as local radial displacements of the detector.
- Δr_2 - Detector misalignments and intrinsic resolution are responsible for this parameter.

The corrections are applied separately on the ID and MS track forming a muon; these two tracks are then recombined using a weighted average of the two momenta to obtain the corrected combined muon momentum.

2.2. Corrections extraction

The correction parameters for ID and MS tracks are estimated with a maximum likelihood fit to data using templates obtained from simulation. In particular, the ID corrections are derived from fitting the invariant mass distribution, $m_{\mu\mu}^{\mathrm{ID}}$, of the J/ψ and Z resonances and are divided in 18 regions in η. The MS corrections, instead, are obtained by fitting in 36 $\eta - \phi$ regions the invariant mass of the J/ψ and Z, as well as the momentum imbalance $\rho = p_{\mathrm{T}}^{\mathrm{MS}}/p_{\mathrm{T}}^{\mathrm{ID}} - 1$ of $Z \to \mu\mu$ candidates. MC simulation is used to build the fit templates for the signal processes and the backgrounds in the Z candidate selection. The background for the J/ψ selection is estimated on data with an analytical fit to the $m_{\mu\mu}$ spectrum.

2.3. Systematic uncertainties

The systematic uncertainties are evaluated by varying several parameters of the template fit. The variations providing the largest impact on the corrections are the following:

Region	Δr_1^{ID}	Δr_2^{ID} [TeV^{-1}]	s_1^{ID} $\times 10^3$
central	$0.0068^{+0.0010}$	$0.146^{+0.039}$	$-0.92^{+0.26}_{-0.22}$
transition	$0.0105^{+0.0018}$	$0.302^{+0.046}$	$-0.86^{+0.30}_{-0.35}$
end-cap	$0.0069^{+0.0121}$	$0.088^{+0.084}$	$-0.49^{+1.17}_{-1.63}$

Table 1: Summary of ID muon momentum resolution and scale corrections, averaged over three main detector regions: central ($|\eta| < 1.05$), transition ($1.05 \leq |\eta| < 2.0$) and end-cap ($|\eta| \geq 2.0$).

Region	Δr_0^{MS} [GeV]	Δr_1^{MS} $\times 10^3$	Δr_2^{MS} [TeV^{-1}]
central, small	$0.115^{+0.083}$	$3.0^{+7.9}$	$0^{+0.21}$
central, large	$0.101^{+0.090}$	$3.4^{+8.1}$	$0^{+0.11}$
transition, small	$0^{+0.080}$	$17.1^{+5.9}$	$0^{+0.22}$
transition, large	$0^{+0.080}$	$19.0^{+4.7}$	$0^{+0.17}$
end-cap, small	$0^{+0.080}$	$2.2^{+7.5}$	$0^{+0.06}$
end-cap, large	$0^{+0.080}$	$17.1^{+5.2}$	$0^{+0.29}$

Table 2: Summary of MS momentum resolution corrections for small and large MS sectors, averaged over three main detector regions: central ($|\eta| < 1.05$), transition ($1.05 \leq |\eta| < 2.0$) and end-cap ($|\eta| \geq 2.0$).

Region	s_0^{MS} [MeV]	s_1^{MS} $\times 10^3$
central, small	$-35^{+17}_{-0.011}$	$+3.57^{+0.38}_{-0.60}$
central, large	$-22^{+7}_{-0.014}$	$-0.22^{+0.37}_{-0.24}$
transition, small	$-32^{+17}_{-0.016}$	$-1.07^{+0.77}_{-0.93}$
transition, large	$-26^{+9}_{-0.017}$	$-1.46^{+0.45}_{-0.57}$
end-cap, small	$-31^{+29}_{-0.031}$	$-0.91^{+1.63}_{-0.91}$
end-cap, large	$-57^{+19}_{-0.021}$	$+0.40^{+1.22}_{-0.50}$

Table 3: Summary of MS momentum scale corrections for small and large MS sectors, averaged over three main detector regions: central ($|\eta| < 1.05$), transition ($1.05 \leq |\eta| < 2.0$) and end-cap ($|\eta| \geq 2.0$).

- Mass window for the Z candidate selection. Non-gaussian smearing effects are accounted for by this variation of ±5 GeV on the $m_{\mu\mu}$ selection.

- Background parametrisation for the J/ψ fit as well as increased muon p_{T} cut (from 8 to 10 GeV) to reduce the weight of low-p_{T} muons.

- Scale parameter for the ID corrections obtained fitting separately the J/ψ and Z samples, to include possible non-linear scale effects.

The final corrections obtained from the fit (including the systematic uncertainties, added in quadrature to the statistical uncertainty) are reported in Tab.1 for the ID smearing and scaling, in Tab.2 for the MS smearing and finally in Tab.3 for the MS scaling.

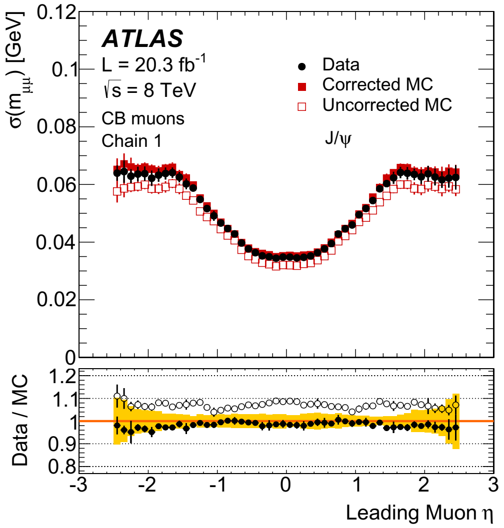

Figure 1: Invariant mass resolution for the $J/\psi \to \mu\mu$ resonance, extracted with the procedure described in Sec.3. The top half shows the resolution for data (black markers), uncorrected simulation (open red markers) and corrected simulation (full red markers). In the bottom half the ratio between data and simulation is shown [3].

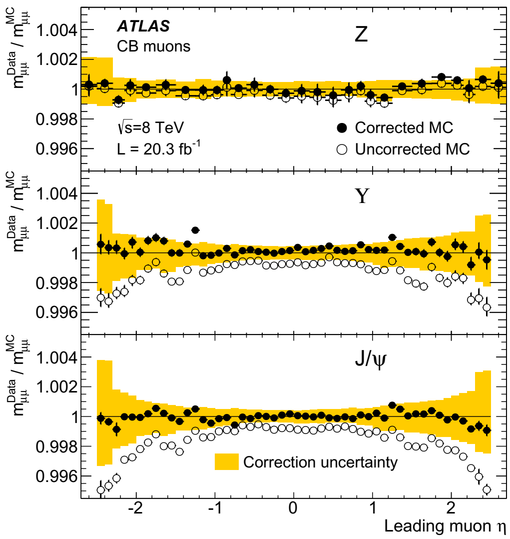

Figure 2: Ratio of the measured reconstructed mass in data and simulation, for three different resonances: Z (top), Υ (centre) and J/ψ (bottom). The ratio is shown both for corrected MC (filled markers) and for uncorrected MC (open markers). The yellow band represents the systematic error associated with the derived corrections. The error bars, on the other hand, represent the statistical and systematic uncertainties on the mass fit (added in quadrature) [3].

3. Measurement of muon momentum scale and resolution

The J/ψ, Z and Υ resonances have been used to measure the muon momentum scale and resolution on both data and simulation and thus validate the corrections extracted with the template fit. The muon momentum resolution is related to the invariant mass resolution by the following equation (if we ignore angular effects and if the momenta of the two muons are similar):

$$\frac{\sigma(m_{\mu\mu})}{m_{\mu\mu}} = \frac{1}{\sqrt{2}}\frac{\sigma(p)}{p} \qquad (2)$$

The mass resolution has been obtained with fits to the invariant mass of the three resonances. For the $J/\psi \to \mu\mu$ and $\Upsilon \to \mu\mu$ the width of the resonance is negligible if compared to the experimental resolution. This allowed the usage of a gaussian model for the J/ψ signal and of a Crystal-Ball model for the Υ signal. In the case of the Z resonance, the true lineshape has been parametrised with a Breit-Wigner function and this has been then convoluted with a gaussian function to measure the experimental resolution. The results obtained for $J/\psi \to \mu\mu$ events are shown in Fig.1. It is possible to translate these results in terms of the momentum resolution on a single muon using Eq.2: this gives us a resolution of about 1.7% in the central region and at low p_T which increases to about 4% in the forward regions and for high-p_T muons.

The momentum scale is validated by comparing the peak position of the resonances, obtained with the same fit described above. The ratio of the mass peak positions between data and corrected (uncorrected) MC is shown in Fig.2, for the three resonances used. The scale is known with an accuracy of 0.05% in the central region and with an accuracy of 0.2% in the forward regions.

References

[1] ATLAS Collaboration, The ATLAS Experiment at the CERN Large Hadron Collider, JINST 3 (2008) S08003.

[2] ATLAS Collaboration, Measurement of the Higgs boson mass from the $H \to \gamma\gamma$ and $H \to ZZ^* \to 4\ell$ channels with the ATLAS detector using 25 fb^{-1} of pp collision data, Phys.Rev. D90 (2014) 052004.

[3] ATLAS Collaboration, Measurement of the muon reconstruction performance of the ATLAS detector using 2011 and 2012 LHC proton-proton collision data, arXiv:1407.3935.